Applied Catalysis A: General 441–442 (2012) 90–98

Contents lists available at SciVerse ScienceDirect

Applied Catalysis A: General

journal homepage: www.elsevier.com/locate/apcata

Partial hydrogenation of 3-hexyne over low-loaded palladium mono and bimetallic catalysts

M. Juliana Maccarrone[a], Cecilia R. Lederhos[a], Gerardo Torres[a,b], Carolina Betti[a], Fernando Coloma-Pascual[c], Mónica E. Quiroga[a,b,*], Juan C. Yori[a,b]

[a] INCAPE, Instituto de Investigaciones en Catálisis y Petroquímica (FIQ-UNL, CONICET), Santiago del Estero 2654, S3000AOJ Santa Fe, Argentina
[b] Facultad de Ingeniería Química – Universidad Nacional del Litoral, Santiago del Estero 2829, S3000AOJ Santa Fe, Argentina
[c] Facultad de Ciencias, Universidad de Alicante, Apartado 99, E-03080 Alicante, Spain

ARTICLE INFO

Article history:
Received 4 May 2012
Received in revised form 12 July 2012
Accepted 14 July 2012
Available online 20 July 2012

Keywords:
Bimetallic catalysts
Alkyne
Selective hydrogenation
Lindlar

ABSTRACT

Partial hydrogenation of alkynes has industrial and academic relevance on a large scale, especially those with high selectivities. To increase the activity, selectivity and lifetime of low-loaded Pd monometallic catalyst, the development of bimetallic systems has been investigated. In this work Pd mono (Pd/A) and bimetallic catalysts (PdNi/A and WPd/A) supported on γ-alumina with low metal content are prepared and evaluated during the partial hydrogenation of 3-hexyne at mild conditions. XPS, XRD, TPR and hydrogen chemisorption techniques are used for the characterization, suggesting different kind of Pd species on the mono and bimetallic catalysts. Furthermore, XPS results indicate the presence of electron rich and electron-deficient palladium species ($Pd^{\delta-}$ and Pd^{n+}, with δ close to 0 and $0 < n < 2$, respectively), electron-deficient species of nickel (Ni^{n+}, with n close to 2) and of $W^{\rho+}$ (with $\rho < 6$) on the surface of the bimetallic systems. The Lindlar commercial catalyst, commonly used in these types of reactions is used for comparative purposes. Bimetallic catalysts showed higher activities and very similar selectivities (>93%) than the monometallic system and further than the Lindlar catalyst. The rank of activity order is: WPd/A > PdNi/A > Pd/A ≫ Lindlar.

1. Introduction

The design of highly selective catalytic systems for which there is no need to remove undesirable products clearly falls within the postulates of the so-called "Green Chemistry". Thus, in the production of fine chemicals where obtaining a product involves a series of complex reactions steps, is essential to achieve greater selectivity in each step. An interesting case is the use of alkynes as raw material for several processes of fine chemicals. The main attraction of the use of alkynes is attributed to its ability to form new C—C bonds via alkylation. In particular, the stereoselective hydrogenation of non terminal alkynes to give alkenes without the occurrence of geometric isomerization is very useful in these processes. When the isomerization reaction is not carried out, the (*Z*)-alkene (desired product) is mainly formed [1]. Furthermore, as in the case of terminal alkynes, it is also necessary that the catalyst does not promote an over hydrogenation forming the corresponding alkane.

Up to now, practically all the studies were concentrated on the reaction of short chain terminal alkynes. There is however only scarce reports that deal with the selective hydrogenation of long chain non terminal alkynes [2–4]. In particular, partial hydrogenation reaction of 3-hexyne has been relatively little studied in the open literature and generally using supported monometallic or complexes as catalysts [2,5–7]. Moreover, information available in the literature is conclusive regarding the use of high loaded Pd catalyst and low reaction temperatures to obtain the (*Z*)-stereoisomer alkene as the main product. For example, for the hydrogenation of 3-hexyne over Pd/C (1 wt% of Pd) at 298 K Mastalir et al. [2] found a decrease of the selectivity to the (*Z*)-isomer with an increase of the substrate/Pd molar ratio, and reported values of selectivity to the (*Z*)-isomer > 98%, to (*E*)-isomer < 1.4% and to n-hexane < 0.5%. Similar product distribution was informed for Pd/SBA-15, Pd/MCM-48 and Pd/MSU-Al_2O_3 catalysts (1 wt% of Pd) for different substrate/Pd molar ratios by Alvez-Manoli et al. [5]. Furthermore, Marín-Astorga et al. [8] reported high selectivity to (*Z*)-alkene isomer during hydrogenation of aromatic alkynes over 1 wt% Pd catalysts. In turn, Papp et al. [9] also reported high selectivity to (*Z*)-alkene form during partial hydrogenation reactions of alkynes of high molar mass (3-butyn-1-ol, phenylacetylene, 4-octyne and 1-phenyl-1-butyne) over Pd/MCM-41 (1.4 and 5.8 wt% of Pd) catalysts.

* Corresponding author at: INCAPE, Instituto de Investigaciones en Catálisis y Petroquímica (FIQ-UNL, CONICET), Santiago del Estero 2654, S3000AOJ Santa Fe, Argentina. Fax: +54 342 453 1068.
E-mail address: mquiroga@fiq.unl.edu.ar (M.E. Quiroga).

0926-860X/$ – see front matter © 2012 Elsevier B.V. All rights reserved.
http://dx.doi.org/10.1016/j.apcata.2012.07.016

The literature is consistent in that if the (*Z*)-isomer of the alkene is the desired product, it is convenient to use a supported Pd catalyst in order to obtain high activity and selectivity. However, considering that palladium is an expensive metal and high loads are apparently necessary, the final cost of the catalyst for alkyne partial hydrogenation processes is very high. So it is a challenge to explore the feasibility of using lower Pd loadings or cheaper metals as catalysts for the hydrogenation of non terminal alkyne of high molar mass.

Another exciting possibility is to analyze the effect of the addition of another metal to Pd, studying its influence on activity and product selectivity. The addition of a second metal to Pd monometallic catalysts has also been found to improve the catalytic properties in several reactions. These so-called bimetallic catalysts have improved activity, selectivity and stability. Many authors have reported the effect of this second metal as Ni, Ag, Cu, Au, Ge, Sn, Pb, etc., using several supports like γ-Al_2O_3, zeolites, silica, etc. on the performance of palladium-based bimetallic catalysts [9–12]. The most clear example studied since 1954 is the well-known Lindlar catalyst, Pd(5%)/$CaCO_3$ modified with lead, used for the selective hydrogenation of alkynes [13].

In previous contributions of the research group, different low-loaded Pd (W–Pd and Pd–Ni) bimetallic catalysts supported on γ-alumina, were tested for the partial hydrogenation of 1-heptyne, a high molecular weight terminal alkyne [14,15]. It was found that both bimetallic catalysts were more active than the Pd monometallic catalyst presenting high selectivity to 1-heptene (>95%). Pd–Ni catalysts were however less active than the commercial Lindlar catalyst, while bimetallic PdW/Al_2O_3 or WPd/Al_2O_3 were more active.

Based on the above considerations the objectives of this work are: (a) to prepare and characterize catalysts of low Pd content, both monometallic and bimetallic (W–Pd and Pd–Ni) catalysts; (b) to evaluate the activity and selectivity of catalysts during 3-hexyne partial hydrogenation at mild reaction conditions; (c) to evaluate the effect of reaction temperature; and (d) to compare the catalytic performance of these catalysts with commercial Lindlar catalyst.

2. Experimental

2.1. Catalyst preparation

γ-Al_2O_3 Ketjen CK 300 previously calcined in air at 823 K to stabilize its texture (S_{BET}: 180 $m^2\,g^{-1}$) was used as support. Mono and bimetallic palladium catalysts supported over alumina were prepared by the incipient wetness technique. Volume and concentration of the impregnating solutions were adjusted to get 0.4 wt% of Pd, 2.4 wt% of W and 0.9 wt% of Ni, on the final mono and bimetallic catalysts.

An aqueous acid solution of $Pd(NO_3)_2$ (Fluka, Cat. No. 76070) at pH = 1 (with HNO_3) was used to prepare the palladium monometallic catalyst (sample Pd/A). After impregnation catalyst was dried overnight at 373 K and calcined in an air flow at 823 K during 3 h.

On the other hand, part of the Pd/A catalyst batch was impregnated with an aqueous acid solution of $Ni(NO_3)_2{\cdot}6H_2O$ (Fluka, Cat. No. 72253) to prepare the bimetallic catalyst, labeled PdNi/A, and then was dried and calcined in the same way and conditions described for the monometallic Pd/A catalyst.

WPd/A bimetallic catalyst was prepared by successive impregnations using an acid solution of $H_3PO_4{\cdot}12WO_3$ (Fluka, Cat. No. 79690), dried overnight at 373 K and calcined in an air flow at 823 K during 3 h. This calcination temperature used assures the complete elimination of phosphorus from the catalysts [15]. Then, sample was impregnated with an acid aqueous solution of $Pd(NO_3)_2$ (pH = 1 with HNO_3), dried overnight and calcined.

Before its catalytic evaluation, the catalysts were reduced in a hydrogen stream (105 mL min^{-1}) during 1 h at the optimum reduction temperature found earlier: Pd/A at 573 K, PdNi/A at 673 K and WPd/A at 393 K [14,15]. All the catalysts were immediatelly used in the tests reaction after the reduction treatment.

The commercial Lindlar catalyst, 5 wt% of Pd on calcium carbonate and poisoned with lead acetate, was provided by Aldrich (Cat. No. 20,573-7) and was used without any pretreatment for comparative purposes as suggested by other authors for alkyne hydrogenation reactions [16].

2.2. Catalyst characterization

Palladium, tungsten and nickel contents were determined by inductively coupled plasma analysis (ICP) in an OPTIMA 2100 Perkin Elmer equipment.

The hydrogen chemisorption of the metal particles on the catalysts surface was measured at 303 K in a Micromeritics AutoChem II 2920 instrument equipped with a thermal conductivity detector (TCD). 0.2 g of the samples was reduced in situ in a 5% (v/v) hydrogen/argon stream during 1 h at the same reduction temperature used before each catalytic test. This methodology ensures that the results of chemisorption are not masked by the formation of β-PdH phase. The samples were degassed in situ in an argon flow (AGA, 99.99%) and cooled up to 303 K. Then the hydrogen uptake was measured by sending calibrated pulses. The metal dispersion was calculated assuming that: (i) in bimetallic catalysts only Pd chemisorbs hydrogen at room temperature, nor W neither Ni [14,15] and (ii) a chemisorption stoichiometry H:Pd = 1 [17].

The electronic states of surface species were determined by X-ray photoelectron spectroscopy (XPS) in a VG-Microtech Multilab equipment, equipped with a Mg Kα ($h\nu$: 1253.6 eV) radiation and a pass energy of 50 eV. The analysis pressure during data acquisition was 5×10^{-7} Pa. Samples were treated in situ in the presence of a H_2 stream following the same pretreatment conditions for each catalyst. A careful deconvolution of the spectra was made and the areas under the peaks were estimated by calculating the integral of each peak after subtracting a Shirley background and fitting the experimental peak to a combination of Lorentzian/Gaussian lines of 30–70% proportions. The reference binding energy (BE) was C 1 s peak at 284.6 eV.

X-ray diffraction (XRD) measurements of powdered samples were obtained using Shimadzu XD-D1 instrument with a Cu Kα radiation (λ = 1.5405 Å) in the $21 < 2\theta < 49^\circ$ at a scan speed of 0.25 min^{-1}. Samples were powdered and reduced under a hydrogen flow, the samples were put into the chamber of the equipment and then data acquisition was made.

The reducibility of the surface species in all the catalysts were determined by temperature programmed reduction (TPR), using a Micromeritics AutoChem II instrument equipped with a TCD. Samples were pretreated under an oxygen flow stream at 673 K during 30 min, and then they were cooled down up to room temperature under an argon flow. The TPR profiles were obtained increasing the temperature up to 1223 K at 10 K min^{-1} in a 5% (v/v) hydrogen/argon stream.

2.3. Catalytic evaluations

Catalytic reaction tests were carried out in a stainless steel stirred tank batch reactor equipped with a magnetically coupled stirrer with two blades in counter-rotation that was operated at 800 rpm. The inner wall of the reactor was completely coated with PTFE in order to prevent the catalytic action of steel reported by other authors [18]. The reactant 3-hexyne (Fluka, Cat. No. 51950, purity > 98%) was dissolved to a 2% (v/v) in toluene (Merck, Cat. No. TX0735-44, purity > 99%). The tests were performed using the

following conditions: 1.4 bar of hydrogen pressure, between 273 and 323 K reaction temperatures, 60–120 mesh particle size, during 0–200 min. The 3-hexyne/Pd molar ratio used was constant for all the prepared catalysts: S/Pd = 14,360. The commercial Lindlar catalyst was used as a reference at identical operational conditions of temperature, pressure and initial concentration of 3-hexyne, with S/Pd = 1115.

With the object to eliminate external diffusional limitations, experiences were carried out using different stirring speeds in the range of 180–1400 rpm. It was found that at stirring rates higher than 500 rpm, 3-hexyne conversion values remained constant, indicating that external gas–liquid limitations were absent. A stirring rate of 800 rpm was therefore chosen for all the catalytic evaluations. On the other hand and in order to ensure that the catalytic results were not influenced by external and intraparticle mass transfer limitations, the catalyst pellets were milled to samples of different particle size: a fraction bigger than 100 mesh (<150 μm), a fraction of 60–100 mesh (250–150 μm) and pellets of 1500 μm (not milled). The obtained values of 3-hexyne conversion were the same for the two milled fractions indicating the absence of internal diffusional limitations. Then particles with sizes smaller than 250 μm were used in all the tests.

Catalytic evaluations were carried out in duplicates within an experimental error <5%. Reactants and products were analyzed by gas chromatography in a Shimadzu GC-2014 equipment using a flame ionization detector and a GS-GAS PRO capillary column (60 m long, 0.32 mm ID). In order to identify each possible reaction product, pure chromatographic patrons of: 3-hexyne, (*Z*)-3-hexene, (*E*)-3-hexene, (*Z*)-2-hexene, (*E*)-2-hexene and n-hexane, were previously injected according with the reaction network presented in Fig. 1 proposed by Alvez-Manoli et al. [5].

3. Results and discussion

3.1. Catalyst characterization

ICP chemical analysis confirmed the metal loading of each catalyst; these values are shown in Table 1. Dispersions of the prepared catalysts, calculated from the hydrogen chemisorption values, are also included in Table 1. As it was said earlier for the bimetallic catalysts we considered that only the palladium sites were responsible for the hydrogen chemisorption, because W and Ni do not chemisorb H_2 at room temperature. As expected the dispersion of the bimetallic catalysts are lower than that of the monometallic catalyst Pd/A. Also, as a consequence of the order of impregnation of the precursors, PdNi/A catalyst presents the lowest dispersion, indicating the biggest particle sizes The lowest dispersion of PdNi/A could be due to an effect of decoration of Pd particles by Ni species (geometrical effect) [19,20]. The possible decoration of Pd particles by WO_x and NiO_x species is an example of metal-support interaction related to the mobility of support surface species during heat treatments, especially at high temperatures. The difractograms of all the catalysts obtained by XRD measurements (not shown), only presented the typical signals of the gamma phase of alumina: 37.7°, 45.98° and 66.98° [21,22]. Because of the low amount of Pd on the catalysts (ca. 0.4 wt%), well below the detection limit of this technique, the presence of Pd crystallites is undetectable. For bimetallic WPd/A catalyst, the absence of peaks in the region $20° < 2\theta < 30°$ indicates that there is no tungsten oxide present as a crystalline segregated phase. Segregated monoclinic WO_3 crystallites can be detected by XRD for W surface concentrations higher than the corresponding surface saturation value (4.3 W atoms nm^{-2}) [23]. Similarly, the absence of peaks at $2\theta = 30°$, 43.3°, 63.0°, 75.5° and 79.5° in bimetallic PdNi/A catalyst indicates that there is no nickel oxide present as a crystalline segregated phase [24].

Fig. 2 contains the TPR traces of the Pd/A, PdNi/A and WPd/A catalysts. The TPR trace of the Pd monometallic catalyst has a main hydrogen consumption peak at a low temperature (287 K), which can be assigned to the presence of bulk PdO particles that are easily reduced. These particles are agglomerated over the support during the calcination of the catalyst as it has been extensively reported in the related literatures [25–27]. The reduction profile of Pd/A also shows a negative peak at about 339 K that is supposedly due to the issue of H_2 during the decomposition of the β-phase of palladium hydrides (β-HPd) that is formed during the reduction of the PdO particles at low temperatures [17,25–27]. These species interact weakly with the support and therefore Pd can be easily reduced. Reduction can indeed proceed completely at room temperature in a hydrogen atmosphere [28].

Furthermore, up to 500 K the reduction profiles bimetallic of PdNi/A and WPd/A shown in Fig. 2, are very similar to the monometallic Pd/A one, presenting a main peak at 296 and 305 K, respectively, corresponding to PdO reduction and to the formation of the β-PdH phase. The decomposition peak for the β-PdH phase is also present at 307 and 332 K, respectively for PdNi/A and WPd/A. Comparing these profiles with that obtained for Pd/A, in the bimetallics PdNi/A and WPd/A there is a shift of PdO reduction peak to higher temperatures (9 and 18 K, respectively), indicating that the presence of Ni or W modifies the reducibility of Pd. A shift to higher temperatures in general may be related to an interaction or electron transfer between Pd and Ni or Pd and W. Besides, there is shift to lower temperatures of the β-PdH phase decomposition peak (−32 and −7 K respectively for PdNi/A and WPd/A) suggesting that the decomposition of this phase is more easily accomplished when nickel or tungsten are interacting with palladium. These shifts to lower temperatures are indicative of different active sites on the catalysts, suggesting an electronic effect between Pd–Ni–Al_2O_3 or Pd–W–Al_2O_3. Furthermore, as shown in Fig. 2 the bimetallic catalyst PdNi/A has a peak at 621 K, due to the reduction of NiO species with weak metal-support interaction [29–33], and a broad peak with a maximum at 1000 K which is attributed to the reduction of nickel aluminates, $NiAl_2O_4$, showing a strong metal-support interaction [24,30,34]. On the other hand, the high temperature peak (>950 K) of the WPd/A trace is similar to that found in the case of the tungsten monometallic catalyst at high temperatures [20,35] and would therefore be related to the

Table 1
Metal loading, dispersion (D) XPS data of BE and atomic ratios, degree of reduction of palladium (Pdr_{ed}/Pd_{total}).

Catalysts	Metal loading (wt%)			*D* (%)	XPS										Pd_{red}/Pd_{total} (%)
	Pd	W	Ni		Pd $3d_{5/2}$				W $4f_{7/2}$	Ni $2p_{3/2}$	Pd/Al	W/Pd	Ni/Pd	Pb/Pd	
					$Pd^{\delta-}$	Pd	$Pd^{\delta+}$	Pd^{n+}							
Pd/A	0.35			60		334.9					0.015				99.0
PdNi/A	0.37		0.89	18	334.2 (54%)		335.3 (46%)			856.6	0.003		1.3		75.0
WPd/A	0.37	2.37		33	334.5 (92%)			336.2 (8%)	35.0		0.007	1.2			52.0
Lindlar	5						335.2 (69%)	336.9 (31%)			[a]			0.7	–

[a] Pd/Ca = 0.243.

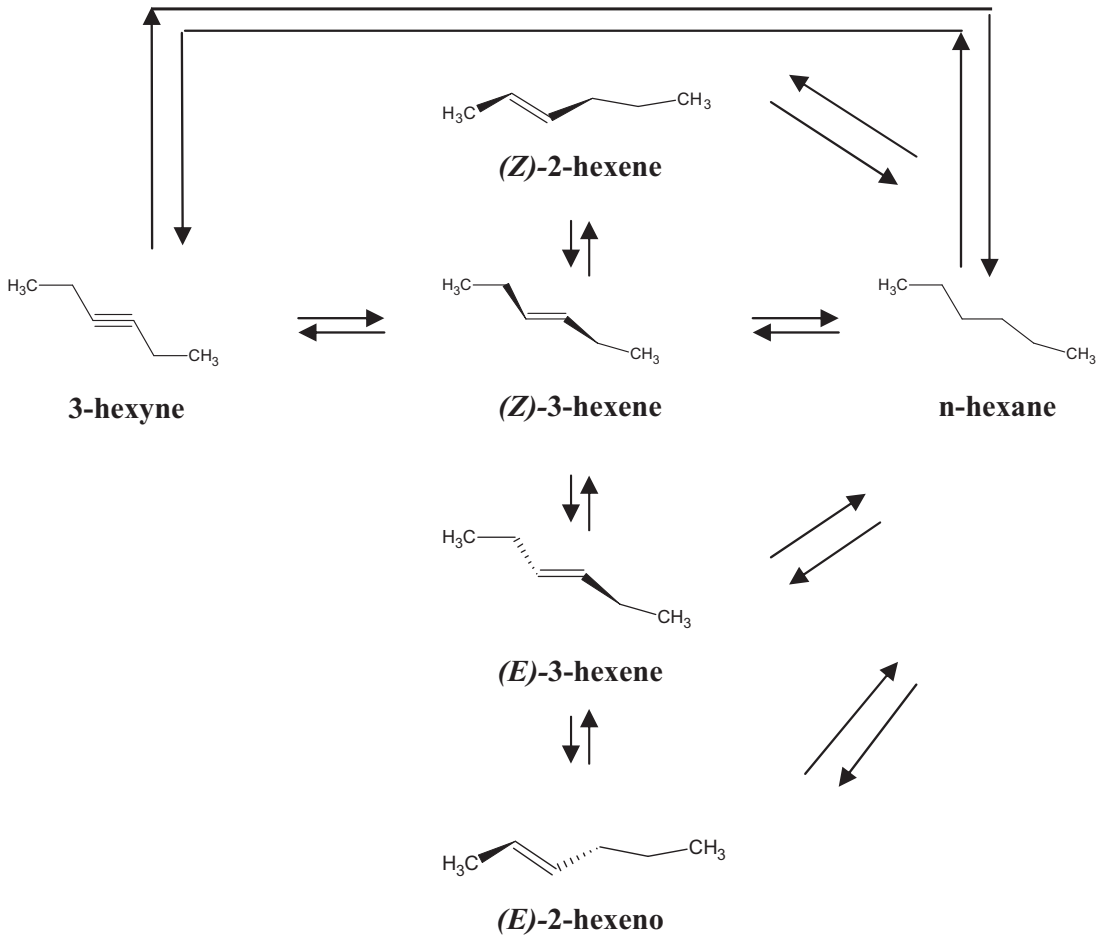

Fig. 1. Scheme of the 3-hexyne reversible hydrogenation reactions.

reduction of amorphous WO_x species. Furthermore, the reduction temperature of oxidized W species is not altered by the presence of Pd, indicating that the reducibility of these superficial species remains very low.

The reduction temperature adopted for palladium mono and bimetallic catalysts (>350 K) during the synthesis of the catalysts ensures the elimination of the β-PdH phase. It must be noted that according to the TPR tests, Pd on the mono and bimetallic catalysts (Pd/A, PdNi/A or WPd/A) is, at least in part, in the Pd metal state after the reduction treatment used before the catalytic tests.

The degrees of reduction of the mono and bimetallic catalysts (Pd_{red}/Pd_{total}, reduced metal amount to total metal amount ratio) were determined by integration of the TPR trace, using a stoichiometry of reduction of one ($H_2/Pd^{2+} = 1$), and are shown in Table 1. These values indicate that Pd is mostly reduced on the monometallic Pd/A catalyst (99%) while in PdNi/A or in WPd/A are only considerably and moderately reduced: 74% and 52%, respectively, suggesting the presence of quite strong Pd–Ni or Pd–W intermetallic interaction in the catalysts; however, the interaction of Pd and Ni with the support or Pd and W with alumina cannot be neglected.

Figs. 3–5 show the XPS spectra of: Pd/A, PdNi/A and WPd/A catalysts. The maximum binding energy (BE) of Pd $3d_{5/2}$, W $4f_{7/2}$ and Ni $2p_{3/2}$ peaks and Pd/Al, W/Pd and Ni/Pd atomic ratios are also listed in Table 1.

As shown in Fig. 3, the Pd $3d_{5/2}$ spectrum of Pd/A catalyst has a peak at 334.9 eV that corresponds to Pd [36]. In the case of the PdNi/A bimetallic catalyst after the deconvolution of the Pd $3d_{5/2}$ spectrum shown in Fig. 4, two signals can be seen at 334.2 eV (54%, at/at) and 335.3 eV (46%, at/at). According to the literature, these values can be assigned to $Pd^{\delta-}$ electron-rich species and slightly electron-deficient palladium species $Pd^{\delta+}$ (with δ close to 0), respectively [36]. The former could be attributed to the formation of metallic bonds or alloy, occurring at low temperatures [37]. Additionally in Fig. 4, for PdNi/A catalyst, the BE of Ni $2p_{3/2}$ peaks appear at 856.6 eV and at 862.9 eV, which are attributed to electron-deficient species (Ni^{n+}, with n close to 2) and to the shake-up

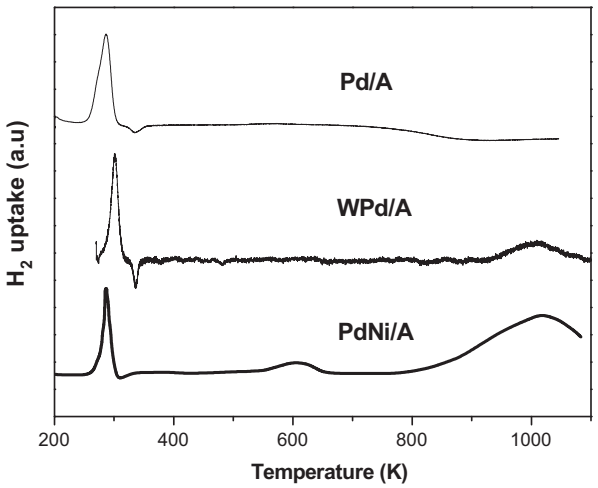

Fig. 2. TPR traces of Pd/A, WPd/A and NiPd/A samples.

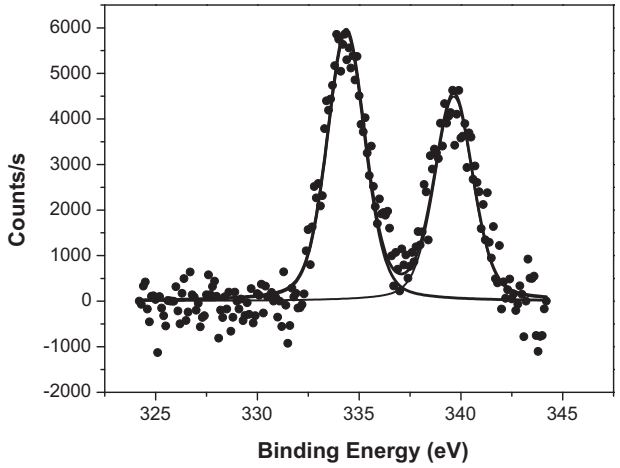

Fig. 3. XPS spectra of the Pd $3d_{572}$ region for Pd/A catalyst.

structure of Ni(II). Ni^{n+} electron-deficient species probably corresponds to different interactions between Ni–Pd or Ni–Al (from the support) [38], or to the formation of intermediate Pd–Ni–Al_2O_3 surface species [14]. Figs. 3–5 are also shown for Pd, the $3d_{3/2}$ peak doublet shifted 5.2 eV respect the $3d_{5/2}$ peak.

Fig. 5 shows the XPS spectra of Pd $3d_{5/2}$ and W $4f_{7/2}$ for bimetallic WPd/A catalyst. The deconvolution of the Pd $3d_{5/2}$ spectrum shown in Fig. 5 displayed two peaks at 334.5 (92%, at/at) and 336.2 eV (8%,

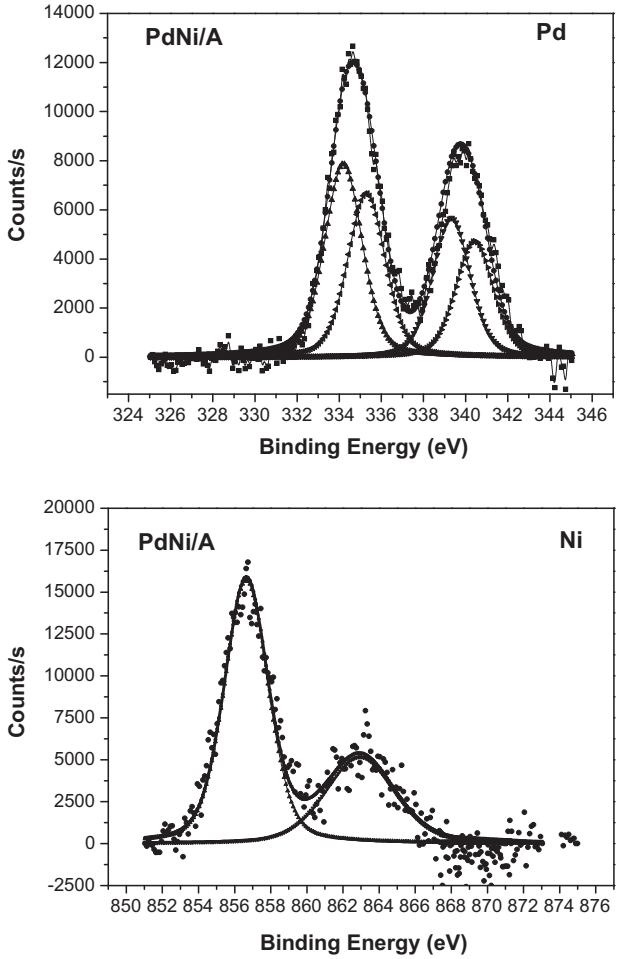

Fig. 4. XPS spectra of PdNi/A catalyst for: Pd $3d_{5/2}$ and Ni $2p_{3/2}$ regions.

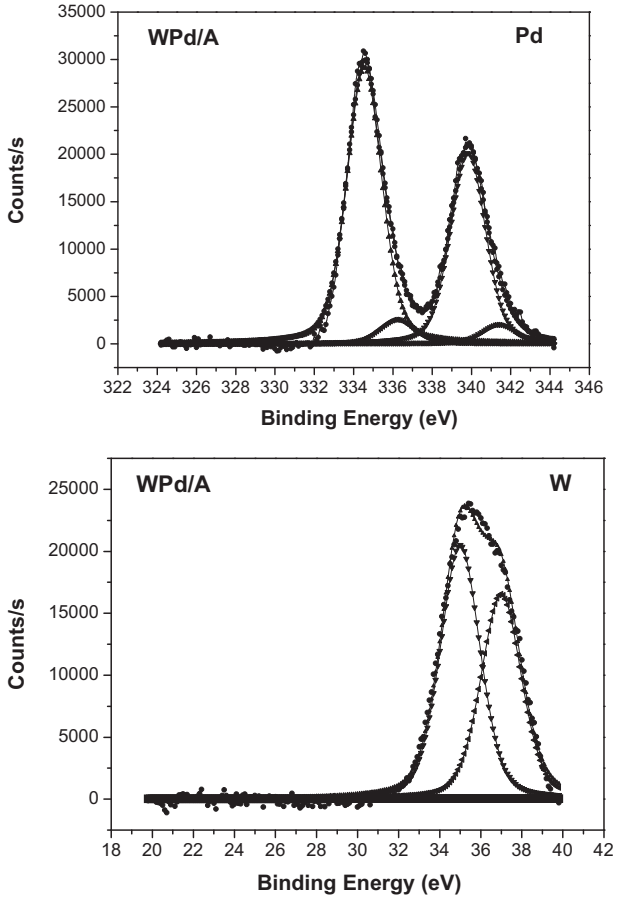

Fig. 5. XPS spectra of WPd/A catalyst for: Pd $3d_{5/2}$ and W $4f_{7/2}$ regions.

at/at) that can be attributed to slightly electron-rich $Pd^{\delta-}$ species (with δ close to 0) and to electron-deficient Pd^{n+} species (with n close to 2), respectively [36]. The spectrum of W $4f_{7/2}$ in Fig. 5 presents a peak at 35.0 eV suggesting the presence of electron-deficient species, $W^{\rho+}$ (with $\rho < 6$) [36]. According to a previous work, this value of BE indicates that tungsten is present on the alumina surface of WPd/A catalyst, with a lower value of BE than on the tungsten monometallic catalyst [15,39]. This pattern and the presence of $Pd^{\delta-}$ electron-rich species can be explained due to the formation of metallic Pd-W bonds or alloys; however this transfer might be due to the formation of intermediate Pd–W–Al_2O_3 surface species [19].

For the Lindlar catalyst, in Fig. 6 are presented the Pd $3d_{5/2}$ and Pb $4f_{7/2}$ spectra. The deconvolution of the Pd $3d_{5/2}$ signal indicates two peaks at 335.2 eV (69%, at/at) and 336.9 eV (31%, at/at), assigned to $Pd^{\delta\pm}$ and electro-deficient Pd^{n+} species (with δ close to 0 and n close to 2), respectively [36]. On the other hand, the deconvolution of Pb $4f_{7/2}$ spectrum shows two peaks at 136.8 eV (20%, at/at) and 138.6 (80%, at/at), attributed to Pb and $Pb(OAc)_2$, respectively.

3.2. Catalytic evaluations

During the catalytic tests the only reaction products observed were (*Z*)-3-hexene, (*E*)-3-hexene and n-hexane, the presence of isomers (*Z*)-2-hexene and (*E*)-2-hexene were not detected. The results obtained for the partial hydrogenation of the internal aliphatic alkyne, 3-hexyne, over Pd/A, PdNi/A, WPd/A and Lindlar catalysts at 303 K are depicted in Fig. 7. In the Figure are plotted the evolution of the concentration of 3-hexyne, (*Z*)-3-hexene, (*E*)-3-hexene and n-hexane as a function of reaction time.

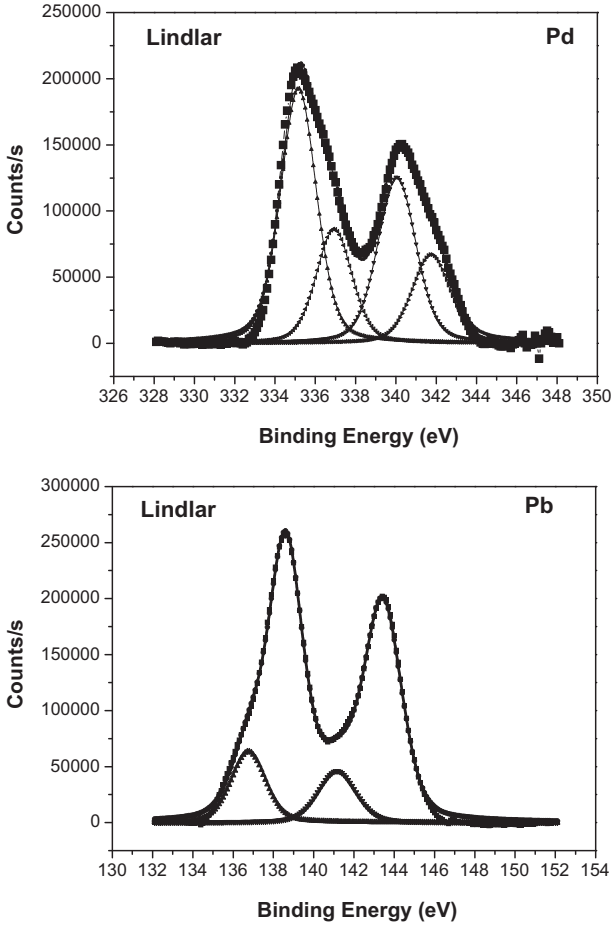

Fig. 6. XPS spectra of Lindlar catalyst for: Pd $3d_{5/2}$ and Pb $4f_{7/2}$ regions.

Fig. 7 shows that at 303 K, all the prepared catalysts present varying degrees of activity for the partial hydrogenation of 3-hexyne. In all the catalytic systems, the concentration profiles obtained experimentally are indicative of irreversible reactions rather than reversible ones shown in Fig. 1. Besides, the partial hydrogenation of 3-hexyne over the Pd-based catalysts results in the predominant formation (*Z*)-3-hexene stereo-isomer accompanied by the production of n-hexane (through over hydrogenation) and of (*E*)-3-hexenes, which may be formed as initial product rather than $(Z) \rightarrow (E)$ isomerization as it can be deduced from the concentration profiles shown in Fig. 7. Also it can be observed that the bimetallic catalysts are more active regarding the monometallic Pd/A at 303 K. Total conversion of 3-hexyne of ca. 100% is reached with PdNi/A and WPd/A, and with the commercial Lindlar catalysts. After the total consumption of the alkyne the isomerization $(Z) \rightarrow (E)$ reaction begin to be predominant rather than the over hydrogenation of the stereo-isomer (not shown for sake of clarity). Furthermore, while 3-hexyne is present in the reaction media, (*Z*)-3-hexene concentration profiles always present an increasing tendency, while the concentration of (*E*)-3-hexene and n-hexane are almost constant all over the reaction tests.

On the other hand, in Fig. 8 are presented the 3-hexyne total conversion vs. time obtained at different reaction temperatures (between 273 and 323 K) for the mono and bimetallic catalysts, and for the Lindlar catalyst. In this figure it is observed that all the catalysts are active in the range of temperatures studied, even at the lowest temperature, 273 K. Experimental results show that, as expected from a kinetic point of view, a beneficial effect of temperature on reaction rate is observed, and the optimum reaction temperature is 323 K because higher total conversions of 3-hexyne are obtained with high selectivity to (*Z*)-3-hexene (≥93%).

For the purpose of comparing the performances of the catalysts, in Table 2 are presented TOF values obtained for the prepared catalysts at 303 K. The same were calculated using initial reaction rates of 3-hexyne calculated from the data plotted in Fig. 8 and dispersion values indicated in Table 1. Initial reaction rate of 3-hexyne was calculated using the following formula:

$$r_A^0 = \frac{V \times C_A^0}{W_{cat}} \times \left(\frac{\partial X_A}{\partial t}\right)_{t=0} \quad (1)$$

where r_A^0 is the initial reaction rate of 3-hexyne [mol g_{Pd}^{-1} min^{-1}]; $(\partial X_A/\partial t)_{t=0}$ the tangent value of the 3-hexyne total conversion vs. time curve at $t=0$; C_A^0 the initial concentration of 3-hexyne [mol L^{-1}]; W_{cat} the mass of catalyst [g]; V the reaction volume [L] and t is the reaction time [min].

TOF values are useful in order to predict possible changes in the nature of the active sites, in this case due to Ni or W interactions with Pd. The calculated TOF values shown in Table 2, indicate the following activity order: WPd/A ∼ PdNi/A ≥ Pd/A. So, the obtained TOF values confirm that different active sites are present on the prepared catalysts. Table 2 also shows product selectivity values for the catalysts at different reaction temperatures. The selectivities are the average values obtained in each experiment while there is 3-hexyne in the reacting media. In all the cases the (*Z*)-alkene stereoisomer is obtained as the main product with a very high selectivity (>93%) and remains approximately constant with temperature, in contrast with results obtained with nickel boride catalyst or homogeneous Pd(II) and Rh(I) complexes [6,7,40]. These values are comparable to those obtained with the commercial Lindlar catalyst. Apparently, this pattern of product selectivities shown in Table 2 is independent of the type of support used (low acidic Al_2O_3 for the prepared catalysts, or basic characteristics of $CaCO_3$ for the Lindlar catalyst) and even of the S/Pd (substrate molecules that react per Pd atom in the catalyst) used the prepared or the Lindlar catalysts during the catalytic tests, in total accordance with Alvez-Manoli et al. [5]. It is well known that in the case of alkyne hydrogenation reactions over palladium supported catalysts, the β-hydride phase may act as a hydrogen source that promotes over hydrogenation, with a consequent decrease in the selectivity to alkene formation [41]. Additionally, Coq and Figueras [42], after analyzing a wide number of papers on the matter of palladium bimetallic catalysts, concluded that the disappearance of the β-PdH phase plays an important role on the activity and selectivity, in the sense of decreasing the alkyne hydrogenation rate to alkanes, and thus increasing the selectivity to alkene formation. For the prepared mono and bimetallic catalysts the palladium β-hydride phase is not present as it is proved by the TPR profiles at the pretreatment reduction temperature adopted. However the existence of steric constraints might not be discarded. Ulan et al. [43] reported that morphological differences in the Pd crystals, that make up the catalyst, affect selectivity in the partial hydrogenation reaction of 3-hexyne. In this regard the authors obtained high selectivities to the (*Z*)-stereoisomer when the alkyne is mainly adsorbed on the (1 1 1) plane of Pd crystals, while the adsorption onto the (1 1 0) plane gave low selectivities to this isomer. The analysis of the activities, expressed as initial reaction rate of 3-hexyne per mass of Pd, shown in Fig. 9, indicates for each catalytic system an increase of r_A^0 with temperature. It can be observed that all the prepared low-loaded mono and bimetallic catalysts, present higher initial reaction rate of 3-hexyne than the high-loaded Lindlar catalyst. Besides, it can be remarked that the addition of W or Ni to Pd catalyst considerably promotes the activity of the monometallic catalyst, without modifying the very high selectivity (typical of Pd). At each reaction temperature evaluated, the following order

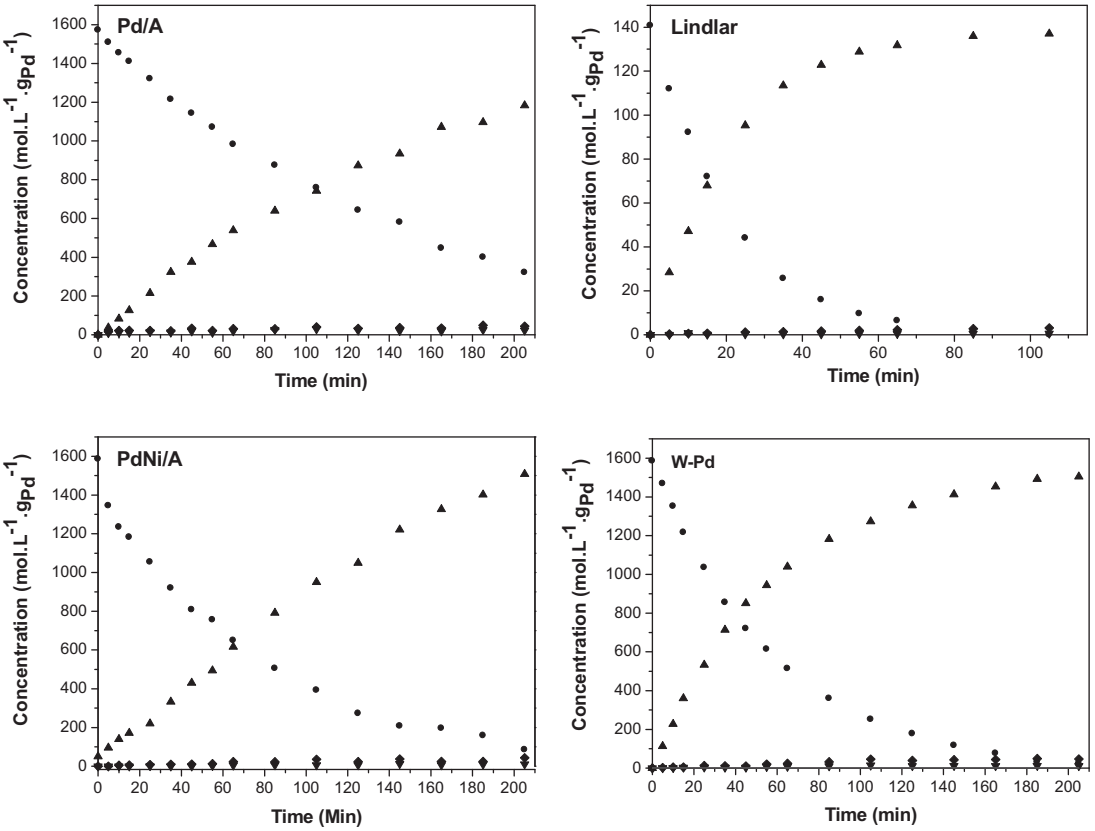

Fig. 7. Evolution of the concentrations of reactant, 3-hexyne (●), and products: (*Z*)-3-hexene (▲), (*E*)-3-hexene (♦) and n-hexane(▼) as a function of time during the partial hydrogenation of 3-hexyne over Pd/A, Lindlar, PdNi/A and WPd/A. Reaction conditions: 1.5 bar of H_2, 303 K, 800 rpm.

of initial reaction rate of 3-hexyne per mass of Pd, was found: WPd/A > PdNi/A ≫ Pd/A ≫ Lindlar. Besides, at the highest evaluated temperature, WPd/A and PdNi/A present initial reaction rate of 3-hexyne, 3.5 and 1.4 times higher than that of Pd/A, while the monometallic initial reaction rate is 2.5 times higher than that of Lindlar catalyst. Furthermore, as for all the catalysts the selectivities are maintained nearly constant with temperature, the yield to the (*Z*)-stereoisomer is maximal at the higher reaction temperature studied (323 K). This means that the optimum is verified at the highest temperature contradicting the opinion of other researchers [6,7,40] who warn about the inconvenience of overcoming 303 K of reaction temperature since that worsens the selectivity to the desired product. The results indicates that higher throughput of product per mass of Pd are obtained for WPd/A (firstly), PdNi/A (secondly) and Pd/A (thirdly) than with commercial Lindlar catalyst.

The dispersion of the prepared catalysts showed that Pd/A catalyst presented the highest *D* value, but as observed this catalyst presented the lowest reaction rate, indicating in this case that a greater capacity for H_2 chemisorption not necessarily means a higher reaction rate. In recent works on kinetic modeling of the selective hydrogenation reaction of 1-heptyne, we have found that on W or Ni monometallic catalysts, that no chemisorbs H_2 at room temperature, the controlling reaction rate step is the dissociative adsorption of H_2 [44,45]; however, on metals with high capacity of H_2 chemisorption, such as Pd, the controlling step is the surface chemical reaction. In the case of Pd it was also verified that an increase in the partial pressure of hydrogen leads to lower values of the reaction rate [45]. As stated in the previous Section, the existence of electron-rich $Pd^{\delta-}$ species on the bimetallic Pd–M catalysts, with M = Ni or W, can be explained due to the formation of metallic bonds or alloys occurring at low temperatures [37,46]; however this transfer might be due to the formation of intermediate Pd–M–Al_2O_3 surface species [14,19]. The causes of the influence of a second metal on the performance of monometallic palladium catalysts are not as straightforward. Alkynes partial hydrogenation reactions are more or less sensitive to geometrical and electronic effects, being the latter the most important ones. The properties of palladium based bimetallic catalysts are related to the preparation method, which affects the electronic and chemical state of Pd and of the second metal, as well as their spaial distribution. As observed by XPS, the species situated on the surface of the prepared catalysts are

Table 2
TOF values estimated at 303 K and products selectivities obtained at different temperatures, 1.4 bar and 800 rpm.

Catalyst	S/Pd	TOF (s^{-1})	Products selectivity (%)								
			(*Z*)-3-hexene			(*E*)-3-hexene			n-hexane		
			273 K	303 K	323 K	273 K	303 K	323 K	273 K	303 K	323 K
Pd/A	14,360	4.73	95.0	94.0	93.0	4.0	4.0	5.0	1.0	2.0	2.0
PdNi/A	14,360	19.40	94.0	94.0	93.0	5.0	5.0	6.0	1.0	1.0	1.0
WPd/A	14,360	19.30	97.0	96.0	95.0	3.0	3.0	4.0	1.0	1.0	1.0
Lindlar	1115		98.0	98.0	97.0	1.7	1.4	2.0	0.3	0.6	1.0

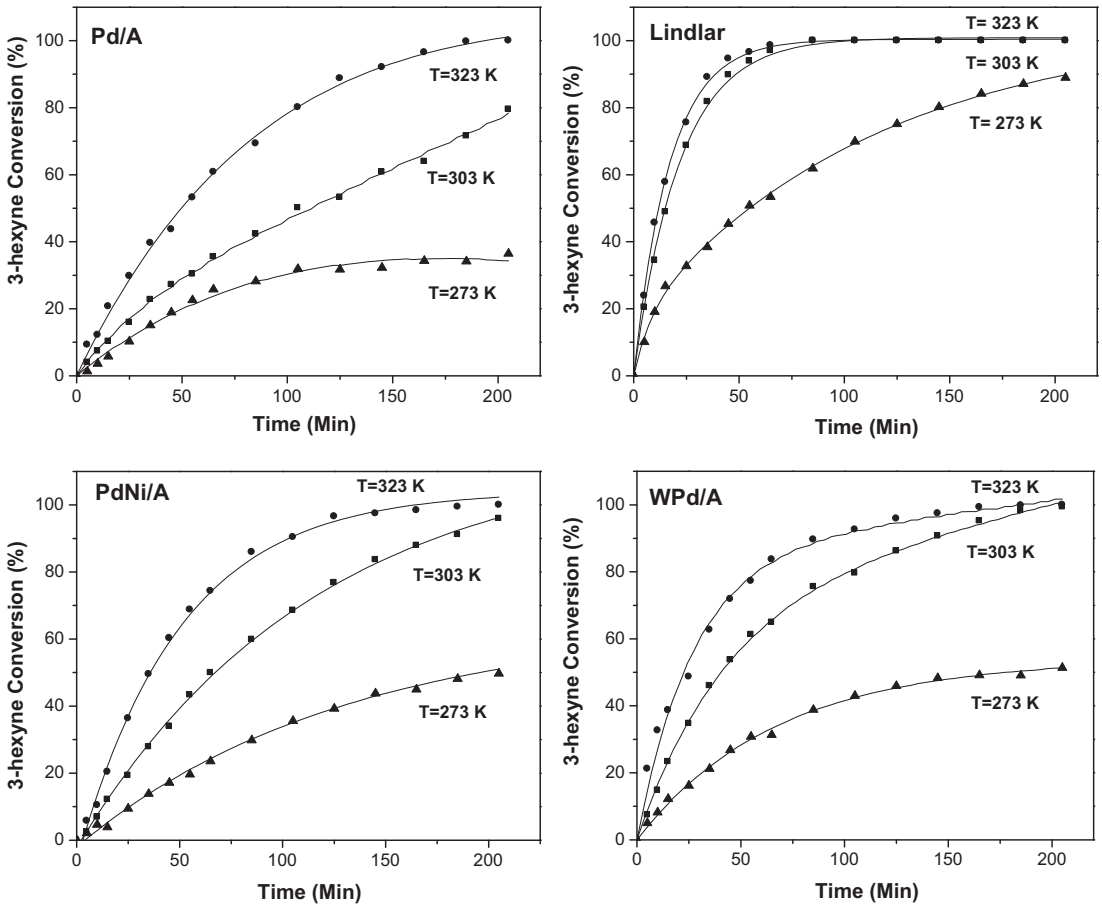

Fig. 8. 3-Hexyne total conversion (%) as a function of time for Pd/A, Lindlar, PdNi/A and WPd/A. catalysts, measured at 1.5 bar and different temperatures: T_1 = 273 K (▲), T_2 = 303 K (■) and T_3 = 323 K (●).

more electron-rich than those present on the surface of the Lindlar catalyst. Even more, the most active catalyst, WPd, presents 92% of electron-rich $Pd^{\delta-}$ species, while the secondly active, PdNi/A, presents a 54% of these species. On the other hand Pd/A presents 100% of palladium totally reduced while there is a 69% of $Pd^{\delta\pm}$ on the Lindlar catalyst. So the characterization results should indicate that, at least in part, the modification of the electronic state of palladium could be responsible for the better catalytic behavior.

It is well known that during hydrogenation reactions metallic centers rich in electrons can cleave the bond in H_2 by means of the interaction of a filled *d* metal orbital with the empty sigma antibonding molecular orbital of H_2 [47]. The rupture of the hydrogen bond is more easily done on metals with a high amount of available electrons in the external *d* orbital, as it is the case of catalysts with electron-rich $Pd^{\delta-}$ species as WPd/A or PdNi/A catalysts (with 92 or 56% of $Pd^{\delta-}$ electron-rich species, respectively), or totally reduced Pd species as Pd/A. This rupture should be less likely on metals with fewer *d* electrons, as in the case of the commercial Lindlar catalyst (with 69% of $Pd^{\delta\pm}$ species, with δ close to 0). Therefore, the differences in activity between the reported catalysts could be attributed, at least in part, to differences in the electronic density of the external *d* orbital of palladium (electronic factor). However, the influence of geometrical effects and/or mixed sites on the activity of bimetallic catalysts cannot be discarded. According to the order of impregnation of Pd during the preparation of each bimetallic catalyst, and because of the low values of hydrogen chemisorption, geometrical effects should be more important on PdNi/A than on WPd/A catalyst, due to an effect of decoration of Pd active sites with NiO_x species [14,15,48]. More work is necessary to continue elucidating the activities enhancement in order to improve the preparation technique of the bimetallic catalysts.

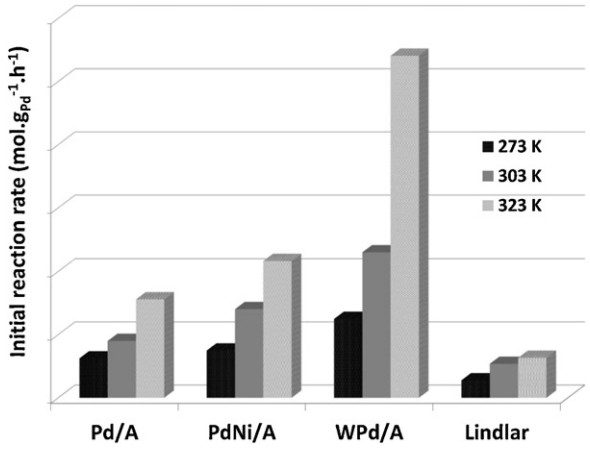

Fig. 9. Activities expressed as initial reaction rates of 3-hexyne per mass of palladium for Pd/A, PdNi/A, WPd/A and Lindlar at 273, 303 and 323 K.

4. Conclusions

Supported low-loaded mono and bimetallic palladium catalysts PdW and WPd were prepared by incipient wetness impregnation of gamma alumina.

The XRD, XPS, TPR and hydrogen chemisorption results reveals that the palladium active sites present in the monometallic Pd/A

catalyst, are quite different respect to those located on the bimetallic PdNi/A or WPd/A catalysts: palladium is totally reduced in Pd/A, while the bimetallic catalysts present electron-rich $Pd^{\delta-}$ and electron-deficient $Pd^{\delta\pm}$ and Pd^{n+} species (with δ close to 0 and n close to 2). Electron-rich species can be explained due to the formation of metallic bonds or alloys occurring at low temperatures, however the formation of intermediate Pd–M–Al_2O_3 surface species cannot be discarded.

Activity results indicate that higher throughput of product are obtained for WPd/A (firstly), PdNi/A (secondly) and Pd/A (thirdly) than with commercial Lindlar catalyst. All the catalysts are active in the range of temperatures studied, 273–323 K, even at the lowest temperature. The selectivities remained approximately constant with temperature, besides, in all the cases the (*Z*)-alkene stereoisomer is obtained as the main product with a very high selectivity comparable to that obtained with the commercial Lindlar catalyst. The optimum reaction temperature is 323 K as higher total conversions of 3-hexyne are obtained with high selectivity to (*Z*)-3-hexene ($\geq$93%). The higher activity of the bimetallic catalyst is related to an electronic effect originated by the superficial electron-rich species. However, the influence of geometrical effects and/or mixed sites cannot be neglected.

Nickel and tungsten proved to be good promoters for the palladium monometallic catalyst as it caused an increment in the activity without modifying the high selectivity to (*Z*)-3-hexene characteristic of Pd monometallic catalysts. Besides, the prepared catalysts present the advantages of low Pd loading and low cost of nickel or tungsten precursors, which leads to cheaper and highly active and selective catalysts.

Acknowledgements

The experimental assistance of C.A. Mázzaro and the financial support provided by UNL, CONICET and ANPCyT are greatly acknowledged.

References

[1] R.L. Augustine, Heterogeneous Catalysis for the Synthetic Chemist, Marcel Dekker Inc., New York, 1996 (Chapter 3–16) pp. 41–43, pp. 387–601.
[2] Á. Mastalir, Z. Király, Á. Patzkó, I. Dékány, P. L'Argentière, Carbon 46 (2008) 1631–1637.
[3] A. Jung, A. Jess, T. Schubert, W. Schütz, Appl. Catal. A: Gen. 362 (2009) 95–105.
[4] J.A. Anderson, J. Mellor, R.P.K. Wells, J. Catal. 261 (2009) 208–216.
[5] G. Alvez-Manoli, T.J. Pinnavaia, Z. Zhang, D.K. Lee, K. Marín-Astorga, P. Rodriguez, F. Imbert, P. Reyes, N. Marín-Astorga, Appl. Catal. A: Gen. 387 (2010) 26–34.
[6] D.A. Liprandi, E.A. Cagnola, M.E. Quiroga, P.C. L'Argentière, Catal. Lett. 128 (2009) 423–433.
[7] D.A. Liprandi, E.A. Cagnola, J.F. Paredes, J.M. Badano, M.E. Quiroga, Catal. Lett. 142 (2012) 231–237.
[8] N. Marín-Astorga, G. Pecchi, J.L.G. Fierro, P. Reyes, Catal. Lett. 91 (2003) 115–121.
[9] A. Papp, Á. Molnár, Á. Mastalir, Appl. Catal. A: Gen. 289 (2005) 256–266.
[10] M.P.R. Spee, J. Boersma, M.D. Meijer, M.Q. Slagt, G. van Koten, J.W. Geus, J. Org. Chem. 66 (2001).
[11] W. Huang, J.R. McCormick, R.F. Lobo, J.G. Chen, J. Catal. 246 (2007) 40–51.
[12] J.G. Chen, S.-T. Qi, M.P. Humbert, C.A. Menning, Y.-X. Zhu, Acta Phys.-Chim. Sin. 26 (4) (2010) 869–876.
[13] H. Lindlar, R. Dubuis, Org. Synth. 46 (1966) 89–92.
[14] C.R. Lederhos, J.M. Badano, M.E. Quiroga, P.C. L'Argentière, Coloma-Pascual sF F., Quim. Nova 33 (2010) 816–820.
[15] C.R. Lederhos, M.J. Maccarrone, J.M. Badano, F. Coloma-Pascual, J.C. Yori, M.E. Quiroga, Appl. Catal. A: Gen. 396 (2011) 170–176.
[16] N. Semagina, M. Grasemann, N. Xanthopoulos, A. Renken, L. Kiwi-Minsker, J. Catal. 251 (2007) 213–222.
[17] C.-B. Wang, H.-K. Lin, C.-M. Ho, J. Molec. Catal. A: Chem. 180 (2002) 285–291.
[18] S. Hu, Y. Chen, J. Chin. Chem. Eng. 29 (1998) 387–396.
[19] P.C. L'Argentière, N.S. Fígoli, Ind. Eng. Chem. Res. 36 (1997) 2543–2546.
[20] A.M. Sica, C.E. Gigola, Appl. Catal. 239 (2003) 121–139.
[21] S. Huang, C. Zhang, H. He, Catal. Today 139 (2008) 15–23.
[22] C. Martín, G. Solana, P. Malet, V. Rives, Catal. Today 78 (2003) 365–376.
[23] S. Chan, I. Wachs, L. Murrell, L. Wang, K. Hall, J. Phys. Chem. 88 (1984) 5831–5835.
[24] E. Heracleous, A.F. Lee, K. Wilson, A.A. Lemonidou, J. Catal. 231 (2005) 159–171.
[25] R.M. Navarro, B. Pawelwc, J.M. Trejo, R. Mariscal, J.L.G. Fierro, J. Catal. 189 (2000) 184–194.
[26] G.M. Tonetto, D.E. Damiani, J. Mol. Catal. A Chem. 202 (2003) 289–292.
[27] V. Ferrer, A. Moronta, J. Sánchez, R. Solano, S. Bernal, D. Finol, Catal. Today 107 (2005) 487–492.
[28] A.B. Gaspar, L.C. Dieguez, Appl. Catal. A: Gen. 201 (2000) 241–251.
[29] F. Cardenas-Lizana, S. Gómez-Quero, M.A. Keane, Appl. Catal. A: Gen. 334 (2008) 199–206.
[30] B.W. Hoffer, A. Dick van Langeveld, J.P. Janssens, R.L.C. Bonne, C.M. Lok, J.A. Moulijn, J. Catal. 192 (2000) 432–440.
[31] P. Kim, H. Kim, J.B. Joo, W. Kim, I.K. Song, J. Yi, J. Molec. Catal. A: Chem. 256 (2006) 178–183.
[32] G. Li, L. Hu, J.M. Hill, Appl. Catal. A: Gen. 301 (2006) 16–24.
[33] Z. Hou, O. Yokota, T. Tanaka, T. Yashima, Appl. Catal. A: Gen. 253 (2003) 381–387.
[34] J.A.C. Dias, J.M. Assaf, Appl. Catal. A: Gen. 334 (2008) 243–250.
[35] X. Li, A. Wang, S. Zhang, Y. Chen, Y. Hu, Appl. Catal. A: Gen. 316 (2007) 134–141.
[36] NIST X-ray Photoelectron Spectroscopy Database NIST Standard Reference Database 20, Version 3.5 (Web Version), National Institute of Standards and Technology, USA, 2007.
[37] N.H.H. Abu Bakar, M.M. Bettahar, M. Abu Bakar, S. Monteverdi, J. Ismail, J. Mol. Catal. A: Chem. 333 (2010) 11–19.
[38] F.U. Hillebrecht, J.C. Fuggle, P.A. Bennett, Z. Zolnierek, Phys. Rev. B 27 (1983) 2179–2193.
[39] V.M. Benitez, C.A. Querini, N.S. Fígoli, R.A. Comelli, Appl. Catal. A: Gen. 178 (1999) 205–218.
[40] J. Choi, N.M. Yoon, Tetrahedron Lett. 37 (7) (1996) 1057–1060.
[41] G. Carturan, G. Facchin, G. Cocco, S. Enzo, G. Navazio, J. Catal. 76 (1982) 405–417.
[42] B. Coq, F. Figueras, J. Mol. Catal. A: Chem. 173 (2001) 117–134.
[43] J.G. Ulan, W.F. Maier, D.A. Smith, J. Org. Chem. 52 (1987) 3132–3142.
[44] M.J. Maccarrone, G.C. Torres, C. Lederhos, J.M. Badano, C.R. Vera, M. Quiroga, J.C. Yori, J. Chem. Technol. Biotechnol. (2012), http://dx.doi.org/10.1002/jctb.3778.
[45] M.J. Maccarrone, G.C. Torres, C. Lederhos, J.M. Badano, C.R. Vera, M. Quiroga, J.C. Yori, in: I. Karamé (Ed.), Hydrogenation, InTech, Croacia, 2012, ISBN 980-953-307-355-7 (Chapter).
[46] J. Álvarez-Rodríguez, I. Rodríguez-Ramos, A. Guerrero-Ruiz, A. Arcoya, Appl. Catal. A: Gen. 401 (2011) 56–64.
[47] D.F. Shriver, P.W. Atkins, C.H. Langford, Inorganic Chemistry, 3rd ed., W.H. Freeman and Co., New York, 1994, p. 258.
[48] C. Betti, J. Badano, M.J. Maccarrone, V. Mazzieri, C. Vera, M. Quiroga, Appl. Catal. A: Gen. (2012), http://dx.doi.org/10.1016/j.apcata.2012.06.001.